Indian Journal of Biochemistry & Biophysics
Vol. 56, June 2019, pp.185-192

Molecular simulation and spectroscopic studies on the interaction between perfluorohexadecanoic acid and human serum albumin

Yan-Qiu Zuo, Zhong-Sheng Yi*, Jie Xu, Yue-Fan Rui, Yu-Cheng Wei & Hong-Yan Liu*

Guangxi Colleges and Universities Key Laboratory of Food Safety and Detection, College of Chemistry and Bioengineering, Guilin University of Technology, Guangxi Guilin- 541 004, China

Received 09 October 2018; *revised 06 February 2019*

In the present study, the interaction between Perfluorohexadecanoic acid (PFHxDA) and human serum albumin (HAS) was studied by fluorescence spectroscopy, molecular docking, dynamic simulation and circular dichroism (CD). The interaction character and the effect on human serum albumin conformation were measured by simulating the physiological condition (pH= 7.4). Experiments and simulation results revealed that PFHxDA molecules and HSA have regular fluorescence quenching, and the quenching mechanism is static quenching and non-radiative energy transfer. Thermodynamic analysis revealed the binding behavior was mainly governed by hydrophobic forces. Specific binding site experiments showed that the binding site of PFHxDA was a site I of HSA. The results from the CD spectrum demonstrated that PFHxDA changed the molecular conformation of HSA, which is consistent with the results obtained by molecular docking and dynamic simulation.

Keywords: Circular dichroism, Dynamic simulation, Human serum albumin, Molecular docking, Perfluorohexadecanoic acid, Spectroscopy

Human serum albumin (HSA) is the most abundant protein in human plasma. Its non-glycosylated single-stranded polypeptide contains approximately 585 amino acids and the molecular weight is approximately 66 KD in plasma concentration of up to 42 g/L, accounting for approximately 60% of total plasma protein[1]. Its main roles in the human body include combining and transporting endogenous and exogenous small molecules, maintaining normal osmotic pressure, inhibiting platelet aggregation and anticoagulation and so on[2,3]. Therefore, the interaction between small molecules and HSA is of great significance to pharmacology, toxicology, life sciences, and environmental science.

Perfluorohexadecanoic acid (PFHxDA) is a long chain of perfluorinated compounds that are applied mainly in the field of semiconductor manufacturing and intermediate products can be applied to fire control, plating, and other chemical products[4]. Because of the small fluorine atom radius (1.47Å), electronegativity (4.0), and other special character that make the C-F bond highly polarized, there is large bond energy (484 kJ/mol) and a high degree of thermal stability[5]. Research has shown that perfluorinated compounds are characterized by persistence and bioaccumulation in living things[6]. They are found in higher quantities in living bodies than are other known organochlorine pesticides, dioxins, and other persistent pollutants. They enter the body *via* water, food, respiration, and other intake routes, and are difficult to excrete[7]. In addition, perfluorinated compounds are a class of systemic toxic environmental pollutants to organs that can cause genetic toxicity, reproductive toxicity, neurotoxicity, developmental toxicity and other toxic effects[8].

In the present study, the interaction mechanism between PFHxDA and HSA was studied by spectroscopy and computer simulation. The binding conformation, binding site, stability, and secondary structure of the two were analyzed in a simulated human body environment.

Materials and Methods

Instruments and reagents

The instruments utilized in the present study included a F-7000 FL Fluorescence Spectrophotometer (Hitachi, Japan), TU-1901 dual-beam UV-visible spectrophotometer (Beijing Puxi Device Works), J-810 round dichroism spectrometer (Japan

*Correspondence:
E-mail: yzs@glut.edu.cn; lhyglite@126.com

Spectrophotometer Co., Ltd.), FA1104 electronic analytical balance (China Jiangsu Taixing Electronic Instrument Factory), and a PHS-3C precision pH meter (Shanghai Leici instrument factory).

The reagents utilized in the present study included trimethylol aminomethane-hydrochloric acid (Tris-HCl) buffer solution concentration at 1.0×10^{-6} mol/L, with an adjusted pH of 7.4. HSA (purity ≥ 97%, United States Sigma-Aldrich) stock solution was prepared at a concentration of 1.0×10^{-5} mol/L with the above buffer solution. PFHxDA (purity ≥ 95%, Swiss AD Company) stock solution mixed with Tris-HCl buffer solution prepared at a concentration of 1.0×10^{-3} mol/L, shaken and maintained at 4°C in the dark. Other reagents were analytical grade and experimental water was secondary distilled water.

The analytical calculations were performed on a RedHat Linux 6.4 system on a DELL server. Molecular dynamics simulation was performed by GROMACS 5.0 software, using molecular docking by AutoDock software. The crystal structure of HSA (code: 1N5U) was obtained from the protein database (http://www.rcsb.org/pdb).

Experimental methods

Spectroscopy: Add 1 mL of 1.0×10^{-5} mol/L concentration of HSA solution into a 10 mL colorimetric tube, then use a pipette to add a certain amount of PFHxDA solution, add Tris-HCl buffer solution to the scale line, and shake. At set temperatures of 291 K, 298 K, and 310 K undertake a constant temperature reaction for 10 min. Measure the emission spectrum at 300-500 nm wavelength with a fluorescence spectrometer having a slit width of 5 nm. The UV–visible absorbance spectra were recorded by a TU-1901 absorption spectrophotometer against a solvent as the reference in the wavelength range of 300-450 nm. The circular dichroism (CD) spectra were recorded from 190 to 240 nm equipped with 1.0 cm quartz cells. For the CD studies, the final concentration of HSA was 1.0×10^{-6} mol/L, and the concentrations of the ligands were 0 and 2×10^{-7} mol/L. The secondary structure was determined to apply CD Pro software by the CDSSTR method.

Molecular docking: Using ChemDraw software to draw the small molecule PFHxDA, the MMFF94 force field was selected to minimize the energy optimized structure. All ligands and water in the 1N5U structure were removed during the molecular docking process and then hydrogen atom and charge were added. The amino acid residue TRP214 was selected as the flexible residue, the size of the acceptor box was 70 × 70 × 70, and the lattice spacing was 0.375 Å. By combining the partial energy search with the genetic algorithm, the semi-empirical potential function was applied as the energy scoring function to obtain 10 independent genetic algorithms operations and create the ligand small molecules and protein 1N5U molecular docking. The results obtained were utilized for molecular dynamics modeling.

Molecular dynamics simulation: The dynamic simulation of free state HSA and PFHxDA-HSA complexes with 20 ns was carried out by the GROMACS program. The topological parameters of HSA were created and the topological parameters of the ligands were built by the Dundee PRODRG 2.5 server (http://davapc1.bioch.dundee.ac.uk/cgi-bin/prodrg). Then, the complex was immersed in a cubic box (with a Fourier grid of 70 × 70 × 70) of extended simple point charge water molecules. To release the conflicting contacts, energy minimization was first performed using the conjugate gradient method of 1000 steps and then the steepest descent method for 1000 steps. Molecular dynamics simulation was carried out by the regular system and the isothermal-isobaric system. Finally, the molecular graphics and analysis of the results were shown in LigPlus software[9].

Results and Discussion

Quenching mechanism of interaction between HSA and PFHxDA

Fluorescence spectroscopy

The endogenous fluorescence of proteins is mainly produced by tryptophan[10]. As can be seen from (Fig. 1A), at 298K HSA had a strong fluorescence peak at 352 nm. With an increase in PFHxDA concentration, the fluorescence waveform of HSA was invariable, and the fluorescence intensity showed an obvious blue shift (approximately 2 nm) and a decrease of approximately 124.801. This indicates that the small molecules of PFHxDA enter the hydrophobic cavity of HSA and interact with its endogenous fluorescent amino acid groups, leading to changes in the internal microenvironment of HSA and the quenching of HSA fluorescence.

Determination of HSA fluorescence quenching mechanism and quenching constant by PFHxDA

Fluorescence quenching of proteins can be divided into dynamic quenching, static quenching, and nonradiative

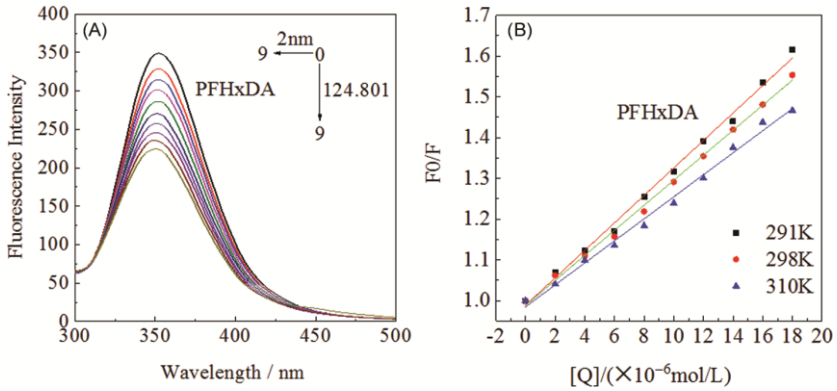

Fig. 1 — (A) Fluorescence quench titration of HSA with increasing PFHxDA concentrations at 298 K cHSA=1.0 × 10^{-5} mol/L, cPFHxDA (1～10)=0,1,2,3,4,5,6,7,8,9 (×10^{-6} mol/L); and (B) The Stern-Volmer curves for the quenching of HSA by PFHxDA at different temperatures

energy transfer according to different mechanisms[11-13]. Data was analyzed by the Stern-Volmer equation to further determine the quenching mechanism of PFHxDA and HSA:

$$F_0/F = 1 + K_q\tau_0[Q] = 1 + K_{SV}[Q] \quad \ldots (1)$$

where, F_0 and F are the fluorescence intensities of HSA solution before and after adding PFHxDA, respectively; [Q] is the concentration of the quencher molecule; K_{sv} is the Stem-Volmer quenching constant; K_q is the bimolecular dynamic quenching rate constant controlled by the diffusion process; and τ_0 is the average life of the fluorescent molecules when the quencher is added. The maximum dynamic quenching rate constant for all types of quenchers on biological macromolecules was 2.0 × 10^{10} L/(mol·s). According to this value, static quenching and dynamic quenching can be judged. If K_q is bigger than 2.0 × 10^{10} L/(mol·s) then it is static quenching, otherwise, it belongs to dynamic quenching.[14-16] The fluorescence quenching data at different temperatures were analyzed by the Stern-Volmer equation and the mechanism of fluorescence quenching can be judged, as shown in (Fig. 1B).

As can be seen from (Table 1), the K_{sv} value of PFHxDA decreased as temperature increased and the K_q value of PFHxDA was greater than 2.0 × 10^{10} L/(mol·s). Analysis of data results showed that the fluorescence quenching of HSA might be due to the complex reaction between the small molecule quencher and the ground state phosphor molecule HSA. Therefore, the quencher enters the HSA cavity and changes the static quench of the original HSA microenvironment.

Nonradiative energy transfer of HSA and PFHxDA

According to the Förster dipole-dipole nonradiative energy transfer theory equation, we can obtain HSA and PFHxDA energy transfer information[17,18]:

Table 1 — The fluorescence quenching constant of PFHxDA - HSA interaction at different temperatures

PFCs	T/K	K_{sv}/(L/mol)	K_q/(L/(mol·s))	R
PFHxDA	291	3.37 × 10^5	3.37 × 10^{13}	0.9977
	298	3.07 × 10^5	3.07 × 10^{13}	0.9985
	310	2.70 × 10^5	2.70 × 10^{13}	0.9966

$$E = 1 - F/F_0 = R_0^6/(R_0^6 + r^6) \quad \ldots (2)$$

$$R_0^6 = 8.79 \times 10^{-25} K^2 N^{-4} \Phi J \quad \ldots (3)$$

$$J = (\sum F(\lambda)\varepsilon(\lambda)\lambda^4\Delta\lambda)/(\sum F(\lambda)\Delta\lambda) \quad \ldots (4)$$

In the equation, E is the energy transfer efficiency; R is the distance between the ligand and the receptor; R_0 is the critical distance when the transfer efficiency is 50%; K^2 is the spatial trend factor and is equal to 2/3; N is the refractive index of the medium, and the average value of the refractive index of water and organic matter is 1.336; Φ represents the fluorescence quantum yield of the protein, and the quantum yield of tryptophan in HSA is approximately 0.15; and the overlap of the fluorescence spectrum of the donor and the absorption spectrum of the receptor is represented by the letter J.

Figure 2 is an overlay of the UV-visible spectra of PFHxDA and the fluorescence spectra of HSA, which shows that the two maps have a certain degree of coincidence. Based on equations 2-4, we can calculate the overlapping integral of two spectral overlapping regions J as 1.16 × 10^{-14} cm^3·L/mol, the energy transfer efficiency of 0.059 and the critical distance R_0 = 2.61 nm. From that, we obtained the binding distance between PFHxDA and HSA tryptophan residues r = 4.16 nm, which is less than 7 nm[19]. The results are consistent with the Förster nonradiative

energy transfer conditions; therefore, the PFHxDA and HSA interaction was *via* the static quenching and nonradiative energy transfer in two ways leading to fluorescence quenching.

The HSA secondary structure changes

The CD spectrum can predict the variation of the secondary structure in the protein of the ultraviolet region (190-240 nm)[20].

As shown in (Fig. 3), the image waveform has a groove at the wavelengths of 216 nm and 222 nm; however, the waveform does not change significantly. Obtained from the literature, α-helix main CD characteristic absorption was at 208 nm and 222 nm, and β-fold characteristic absorption was at 216 nm[20]. Based on analysis of graphical data by CD Pro software after adding PFHxDA (Table 2), the α-helix content of HSA increased from 31.7% to 40.1%; however, the β-fold content decreased from 17.4% to 15.6%. This indicates that when PFHxDA enters HSA, it interacts with HSA residues, which increases the α-helix content in HSA, decreases the β-fold content, drives the internal structure of the protein to shrink and polymerize, and changes the secondary structure of HSA.

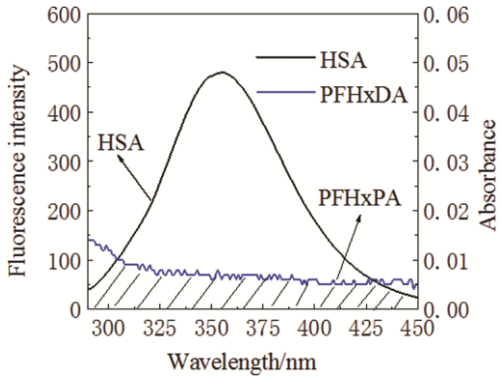

Fig. 2 — The overlap of fluorescence emission spectrum of HSA with the UV-vis absorption spectrum of PFHxDA. T = 298K, CHSA = CPFHxDA = 1.0×10^{-6} mol•L-1

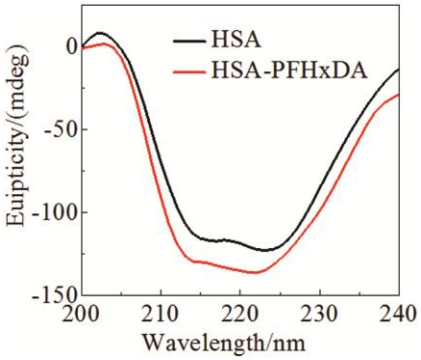

Fig. 3 — The CD spectra of HSA and HSA-PFHxDA complex. The molar ratio of HAS and PFHxDA was 5: 1

Calculation of binding constant and number of binding sites of PFHxDA and HSA

From the above data, PFHxDA and HSA quenching mechanism were determined to be static quenching and nonradioactive energy transfer. The static quenching process can be analyzed by the static quenching equation[21]:

$$\lg(F_0 - F)/F = \lg K_a + n\lg[Q] \quad \ldots (5)$$

where F_0 is the initial fluorescence intensity of the HSA solution; F is the fluorescence intensity of the HSA solution after adding PFHxDA; Q is the concentration of perfluorocarboxylic acid quencher; K_a is the binding constant of quencher with HSA and n is the binding site number. From the linear equations of log [(F_0-F) / F] and log [Q], it can be concluded that the slope of the straight line is the number of binding sites, and the intercept is log K_a. Based on equation (5), the double logarithmic curve of HSA fluorescence quenching of PFHxDA at different temperatures was obtained. The number of binding sites n and the apparent binding constant K_a were obtained from the slope and intercept of the straight line (Table 3).

It can be seen from (Table 3), that the binding constant of PFHxDA and HSA was above 1.0×10^5 L/mol, which indicates that the complex produced by the reaction had good stability. At the same time, it can explain that PFHxDA can be stored and transported in HSA, *i.e.*, PFHxDA has a strong toxic side effect of proof. The value of n was approximately equal to 1, indicating that PFHxDA and HSA have only one binding site. From the literature (6-8), thermodynamic constants can determine the type of interaction

Table 2 — CD Pro software analysis results for HSA secondary structure

	CD Pro software/%				
	Helix	Stand	Turns	Unordered	Sum
HSA	31.7	17.4	17.7	33.1	99.9
HSA-PFHxDA	40.1	15.6	19.6	24.5	99.8

Table 3 — The apparent binding constants K_a and binding sites n of PFHxDA - HSA at different temperatures

PFCs	T/K	K_a/(L/mol)	n	R
PFHxDA	291	3.17×10^5	1.0056	0.9966
	298	2.80×10^5	1.0174	0.9969
	310	1.93×10^5	1.1084	0.9981

between small molecules of contaminants and biological macromolecules[22,23].

$$ln(K_2/K_1) = \Delta H(1/T_1 - 1/T_2)/R \quad \ldots (6)$$

$$\Delta G = -RT\ln K \quad \ldots (7)$$

$$\Delta S = -(\Delta G - \Delta H)/T \quad \ldots (8)$$

The $\Delta H < 0$, $\Delta H > 0$, and $\Delta S > 0$ of the interaction between PFHxDA and HSA can be construed from (Table 4). It can be deduced that the process of interaction between PFHxDA and HSA is a spontaneous process, and the interaction between PFHxDA and HSA is mainly a hydrophobic force.

Competitive experiments of PFHxDA and HSA binding sites

A competitive experiment is an effective and quick method for judging the binding and integration of small molecules and proteins. HSA can be divided into three functional areas, with each functional area containing two sub-areas, A and B. In this section, warfarin, and ibuprofen were utilized as fluorescent probes to label HSA Site I and Site II, respectively[24].

Table 4 — The thermodynamic parameters of PFHxDA - HSA interaction at different temperatures

PFCs	T/K	ΔH/(kJ/mol)	ΔG/(kJ/mol)	ΔS/(J/(mol·K)
PFHxDA	291	13.19	−24.69	130.2
	298		−25.60	
	310		−26.87	

The binding positions of PFHxDA and HSA can be calculated from the experimental data. The results of the competitive experiments can be calculated from the modified Stern-Volmer equation[22]:

$$\frac{F_0}{F_0 - F} = \frac{1}{f} + \frac{1}{f \cdot K_a \cdot [Q]} \quad \ldots (9)$$

The *f* in the equation is the correction factor. Based on equation (9), the change in the bound constant of warfarin was relatively large, K_a (blank, 1.86×10^5 L/mol) and after addition of warfarin, K_a (warfarin, 3.57×10^4 L/mol), the binding constant was reduced by an order of magnitude. The binding constant of K_a (ibuprofen, 1.17×10^5 L/mol) also increased when ibuprofen was added; however, this was smaller than that of warfarin. Therefore, the experimental results showed that PFHxDA was mainly bound to HSA site I.

Molecular docking of PFHxDA and HSA

Molecular docking can theoretically study the binding of small molecules to proteins and can show two types of interactions[25]. Molecular docking was performed using the semi-flexible software AutoDock[26]. To visually understand the interaction between small molecules and the surrounding residues of HSA, the interaction between the ligand and the receptor was simulated by molecular docking at the molecular level. The docking results are shown in (Fig. 4).

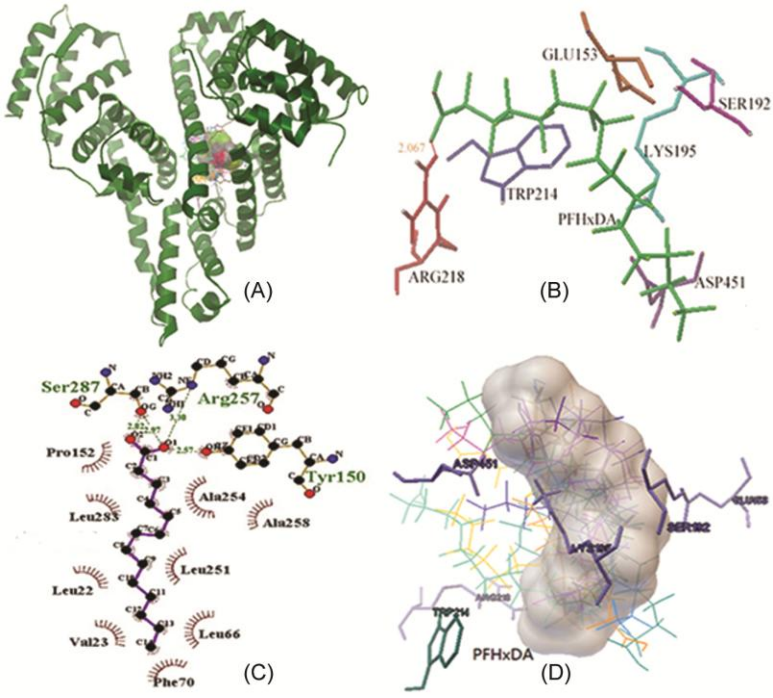

Fig. 4 — Molecular docking results of PFHxDA and HSA. (A) HSA combined with PFHxDA; (B) PFHxDA binds to the residues around HSA site; (C) hydrophobic / hydrophilic action between PFHxDA and HSA; and (D): The overlap of PFHxDA for all conformations in 10 docking simulations

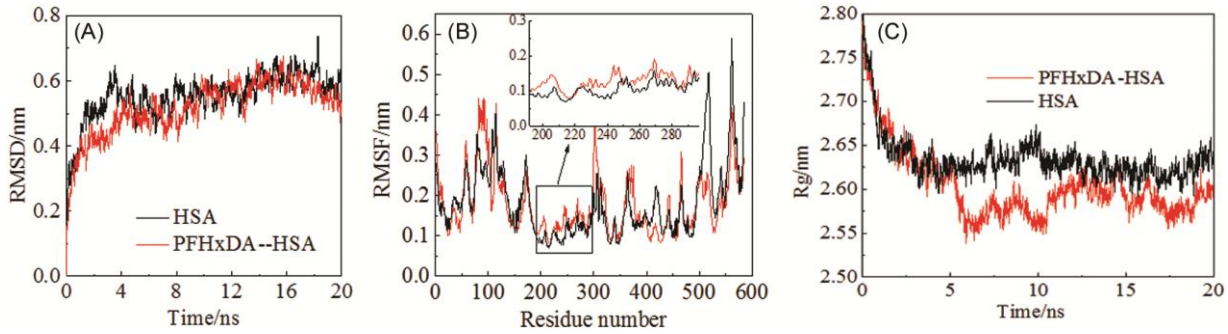

Fig. 5 — Dynamic Simulation of PFHxDA and HAS: (A) RMSD of free HSA and PFHxDA – HAS complex during the 20 ns MD simulation; (B) RMSF of free HSA and PFHxDA – HAS complex; and (C) Time evolution of the protein of Gyration

As can be seen from the docking results in (Fig. 4A), PFHxDA binds to HSA at the cavity of the site I (warfarin site). In (Fig. 4B), we can roughly understand the location of PFHxDA and residues near site I. At the same time, PFHxDA and ARG218 residues form hydrogen bonds with a hydrogen bond distance of 2.067 Å, which has an important effect on the stability of the complex[27]. As shown in (Fig. 4C), the majority of the amino acid residues around PFHxDA are hydrophobic amino acids (Leu 22, Val 23, Leu 66, Phe 70, Pro 152, Leu 251, Ala 254, Leu 283, and so on); therefore, there is a strong hydrophobic interaction. This is consistent with the previous thermodynamic narrative results. (Fig. 4D) shows the overlap of PFHxDA for all conformations in 10 docking simulations.

Molecular docking revealed that PFHxDA binds to HSA at the site I, and the combination of small molecules change the secondary structure of the original HSA. The experimental results are highly consistent with CD spectroscopy and competitive experiments.

Dynamics simulation experiments

Molecular dynamics simulation is an important tool for understanding the physical basis of the structure and function of biological macromolecules. The dynamics simulation of free (HSA) and composite (PFHxDA-HSA) molecules was carried out by GROMACS 5.0 software to analyze the combination[28]. The conformational change of the structure was analyzed by calculating the parameters such as root mean square deviation, root mean square fluctuation, rotation radius (Rg), and so on[29,30].

Root mean square deviation was utilized to describe the statistical value of the system constants to measure the stability of the system. As (Fig. 5A) shows, we performed a 20 ns simulation. It was observed that based on the root mean square deviation between PFHxDA-HAS and HSA, the complex formed by PFHxDA-HSA was smaller than that of HSA, which indicated that the complex formed by PFHxDA-HSA was more stable.

Root mean square fluctuation can be utilized to describe the fluctuation of the two systems relative to the equilibrium position. As shown in (Fig. 5B), HSA and PFHxDA-HSA at the position I (residues 196-297) had different fluctuation to other locations, and small molecules combined with HSA resulted in a change in the surrounding microenvironment. The results obtained are in good agreement with the molecular docking and CD spectra in the previous section.

Rotation radius can be utilized to measure the tightness of the molecular structure. As shown in (Fig. 5C), the radius of rotation of the free HSA molecule was relatively stable with respect to the complex. The radius of the complex formed by PFHxDA and HSA decreased rapidly with time and was lower than that of the free HSA molecule after a certain period. This indicates that the amino acid structure of the constituent proteins was contracted after the small molecule interacted with the protein, which made the secondary structure of the HSA change, further proving the accuracy of the CD spectrum.

Conclusion

In the present study, the stability, secondary structure, and thermodynamics of complexes were obtained from the specific binding sites by spectroscopy (fluorescence spectroscopy, UV-vis spectra, and CD spectroscopy) and computational simulations (molecular docking and molecular dynamics simulation) function and so on several aspects elaborated of the small molecule PFHxDA and HSA interaction characteristics. Experimental results demonstrated that PFHxDA caused fluorescence quenching of HSA by static quenching and nonradiative energy transfer. The CD

spectrum results revealed that the secondary structure of HSA changed. The results of the thermodynamics analysis showed that the hydrophobic interaction and electrostatic attraction were the main forces to maintain the complex of PFHxDA and HSA, and the formation of H-bonds decreased the hydrophilicity and increased the hydrophobicity, thus stabilizing the structures. The competition experiment showed that the binding site of PFHxDA was a site I of HSA, which was consistent with the result of molecular docking, thus improving the accuracy of the experiment. Finally, the various experimental methods utilized in the present study provide more reference for the toxicity of fluorinated organic compounds and perfluorinated compounds.

Acknowledgment

This research was financially supported by the National Natural Science Foundation of China (No. 21467006 and 21866011) and the Guangxi Natural Science Foundation of China (NO. 2017GXNSF AA198354).

References

1 Li J, Li J & Jiao Y, Spectroscopic analysis and molecular modeling on the interaction of jatrorrhizine with human serum albumin (HSA). *Spectrochim Acta A Mol Biomol Spectrosc*, 118 (2014) 48.

2 Huang BX, Kim HY & Dass C, Probing three-dimensional structure of bovine serum albumin by chemical cross-linking and mass spectrometry. *J Am Soc Mass Spectrom*, 15 (2004) 1237.

3 Sun Q, Yang H & Tang P, Interactions of cinnamaldehyde and its metabolite cinnamic acid with human serum albumin and interference of other food additives. *Food Chem*, 243 (2018) 74.

4 Pan YY, Shi YL & Cai YQ, Determination of perfluorinated compounds in soil, Sediment and sludge using HPLC-MS/MS. *Environ Chem*, 29 (2010) 519.

5 Moody CA, Kwan WC, Martin JW, Muir DCG & Mabury, SA, Determination of perfluorinated surfactants in surface water samples by two independent analytical techniques: liquid chromatography/tandem mass spectrometry and 19F NMR. *Anal Chem*, 73 (2001) 2200.

6 Cao Y, Zhang YH & Lei CW, Environmental Pollution and Ecological Toxicity of Perfluorinated Chemicals: a Riview. *J Environ Health*, 29 (2012) 561.

7 Zhang H, Shi Z, Liu Y, Wei Y & Dai J, Lipid homeostasis and oxidative stress in the liver of male rats exposed to perfluorododecanoic acid. *Toxicol Appl Pharmacol*, 227 (2008) 16.

8 Hickey NJ, Crump D, Jones SP & Kennedy SW, Effects of 18 perfluoroalkyl compounds on mRNA expression in chicken embryo hepatocyte cultures. *Toxicol Sci*, 111 (2009) 311.

9 Wu ZW, Yi ZS, Dong L, Yang LL, Yang W & Zhang AQ, Combined simulation and multispectral investigation on the effect of 2′-OH-BDE-28 on the structure of HSA. *Asian J Ecotoxicol*, 11 (2016) 159.

10 Farahani BV, Barddajee GR & Rajabi FH, Study on the interaction of Co(Ⅲ) DiAmsar with serum albumins: Spectroscopic and molecular docking methods. *Spectrochim Acta A Mol Biomol Spectrosc*, 135 (2015) 410.

11 Wang YM, Zhang C, Li J, Li ZX & Gong MX, Interaction of Antimalarial Components Combination from artemisia annual, with Bovine Serum Albumin. *Chem J Chinese U*, 35 (2014) 309.

12 Ghalandari B, Divsalar A, Saboury AA, Haertlé T &Parivar K, Spectroscopic and theoretical investigation of oxali–palladium interactions with β-lactoglobulin. *Spectrochim Acta A Mol Biomol Spectrosc*, 118 (2014) 1038.

13 Dong L, Yi ZS, Wu ZW, Wang HY & Zhang AQ, Mechanism study on the interaction between 2'-hydroxy-2,4-dibromo diphenyl ethers and human serum albumin based on spectroscopic methods and computional Simulations. *Chem J Chinese U*, 36 (2015) 516.

14 Ishtikhar M, Rabbani G & Khan RH, Interaction of 5-fluoro-5′-Deoxyuridine with human serum albumin under physiological and Non-physiological condition: A Biophysical Investigation. *Colloids Surf B Biointerfaces*, 123 (2014) 469.

15 Zhou FH, Bi SY, Wang Y & Zhao TT, Investigation on the interaction between cryptotanshinone and human serum albumin by multi-spectral technologies. *Phys Testing Chem Anal B*, 52 (2016) 318.

16 Cui FL, Zhang QZ, Yan YH, Yao XJ, Qu GR & Lu Y, Study of characterization and application on the binding between 5-iodouridine with HSA by spectroscopic and modeling. *Carbohydr Polym*, 73 (2008) 464.

17 Fani N, Bordbar AK & Ghayeb Y, Spectroscopic, docking and molecular dynamics simulation studies on the interaction of two Schiff base complexes with human serum albumin. *J Lumin*, 141 (2013) 166.

18 Farooqi MJ, Penick MA, Negrete GR & Brancaleon L, Interaction of human serum albumin with novel 3,9-disubstituted perylenes. *Protein J*, 32 (2013) 493.

19 Zhao J, Zhu XW, Xu T & Yin DQ, Structure-dependent activities of polybrominated diphenyl ethers and hydroxylated metabolites on zebrafish retinoic acid receptor. *Environ Sci Pollut Res*, 22 (2015) 1723.

20 Khan SN, Islam B, Yennamalli R, Sultan A, Subbarao N & Khana AU, Interaction of mitoxantrone with human serum albumin: Spectroscopic and molecular modeling studies. *Eur J Pharm Sci*, 35 (2008) 371.

21 Hu YJ, Liu Y, Wang JB, Xiao XH & Qu SS, Study of the interaction between monoammonium glycyrrhizinate and bovine serum albumin. *J Pharm Biomed Anal*, 36 (2004) 915.

22 Gong QL, Hu XG, Fang GY & Li XH, Study of the interaction between 8-azaguanine and bovine serum albumin using optical spectroscopy and molecular modeling methods. *J Mol Model*, 18 (2012): 493.

23 Meti MD, Byadagi KS, Nandibewoor ST & Chimatadar SA, Mechanistic studies of uncatalyzed and ruthenium(III)-catalyzed oxidation of the antibiotic drug chloramphenicol by hexacyanoferrate(III) in aqueous alkaline medium: a comparative kinetic study. *Monatsh Chem*, 41 (2014) 2377.

24 He W, Li Y, Xue C, Hu Z, Chen X & Sheng F, Effect of Chinese medicine alpinetin on the structure of human serum albumin. *Bioorg Med Chem*, 13 (2005) 1837.

25 Ganeshpurkar A & Saluja A, *In silico* interaction of rutin with some immunomodulatory targets: a docking analysis. *Indian J Biochem Biophys*, 5 (2018) 88.

26 Prabhakar MM, Manoharan S, Ignacimuthu S & Stalin A, *In silico* docking analysis to explore the proapoptotic and anti cell proliferative potential of ferulic acid. *Indian J Biochem Biophys*, 53 (2017) 17.

27 Sinisi V, Forzato C, Cefarin N, Navarini L & Berti F, Interaction of chlorogenic acids and quinides from coffee with human serum albumin. *Food Chem*, 168 (2015) 332.

28 Singh K, Jadhao RS, Maharana J,Samal KC, Pradhan SK & Rout GR, Structural investigation of Indica rice (*Oryza sativa* L.) DREB1AP2 domain in response to GCC-BOX DNA: an insight from molecular dynamics. *Indian J Biochem Biophys*, 54 (2017) 47.

29 Scott KA, Bond PJ, Ivetac A, Chetwynd AP, Khalid S & Sansom MS, Coarse-grained MD simulations of membrane protein-bilayer self-assembly. *Structure*, 16 (2008) 621.

30 Philippopoulos M, Mandel AM, Palmer AG & Lim C, Accuracy and precision of NMR relaxation experiments and MD simulations for characterizing protein dynamics. *Proteins*, 28 (1997) 481.